ELSEVIER

Journal of Photochemistry and Photobiology A: Chemistry 116 (1998) 127–133

Journal of Photochemistry and Photobiology A:Chemistry

Ion-responsive fluorescent compounds
V. Photophysical and complexing properties of coumarin 343 linked to monoaza-15-crown-5

J.-L. Habib Jiwan [a], C. Branger [b], J.-Ph. Soumillion [a], B. Valeur [b,c,*]

[a] *Laboratoire de Photochimie et Chimie Organique Physique, Université catholique de Louvain, 1 Place Louis Pasteur, B-1348 Louvain-la-Neuve, Belgium*
[b] *Laboratoire de Photophysique et Photochimie Supramoléculaires et Macromoléculaires (CNRS URA 1906), Département de Chimie, ENS-Cachan, 61 Av. du Président Wilson, F-94235 Cachan cedex, France*
[c] *Laboratoire de Chimie Générale, Conservatoire National des Arts et Métiers, 292 rue Saint-Martin, F-75003 Paris, France*

Received 11 February 1998; accepted 22 April 1998

Abstract

The photophysical and complexing properties of a fluoroionophore consisting of coumarin 343 linked to monoaza-15-crown-5 are reported in acetonitrile and ethanol. The amide link between the coumarin and the crown precludes pH sensitivity of the tertiary amine bridging group. Upon complexation by calcium and magnesium cations, the photophysical properties undergo marked changes, whereas the effects are insignificant or very weak with alkali metal ions. I.R. spectra were recorded in deuterated acetonitrile in order to unravel the participation of the carbonyl groups in the complexation. The stoichiometry of the complexes is 1:1 apart from the case of complexation with calcium in acetonitrile where two complexes can be formed. The stability constants of the complexes were determined in acetonitrile and ethanol.
© 1998 Elsevier Science S.A. All rights reserved.

Keywords: Supramolecular photochemistry; Ion recognition; Fluorescence; Coumarin

---

1. Introduction

Fluoroionophores consisting of fluorophores linked to complexing units have been the object of considerable interest with the aim at selective detection of metal ions, especially cations of biological interest [1–3]. The principles of fluoroionophore design have been reviewed [4]. The changes in photophysical properties on cation binding may arise from various photoinduced processes such as electron transfer [5], charge transfer [6], excimer formation or disappearance [7], and energy transfer [6].

We have previously described the photophysical and complexing properties of various fluoroionophores in which coumarin 153 is linked to monoaza- and diazacrowns via a methylene bridge [8–12]. For example, the formula of C153-crown(O4) is the following.

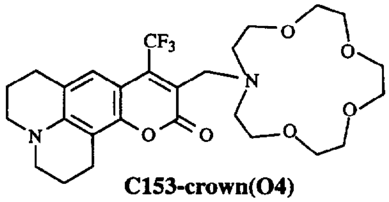

C153-crown(O4)

It was demonstrated that the carbonyl group of the coumarin moiety participates in the complexation which results in high stability constants of the complexes. Moreover, this carbonyl group plays the role of an electron-withdrawing group conjugated with an electron-donating group, i.e., the nitrogen atom in position 7. Consequently, cation binding results in enhancement of the photoinduced charge transfer between these conjugated groups which leads to marked photophysical changes. However, apart from some interesting selective photophysical effects, the selectivity was in general found to be poor owing to the flexibility of the crown as well as around

---

[*] Corresponding author.

1010-6030/98/$ - see front matter © 1998 Elsevier Science S.A. All rights reserved.
PII S1010-6030(98)00286-X

the spacer between the dye and the crown; moreover, the nitrogen atom of the crown is easily protonable.

In order to improve the selectivity and avoid pH sensitivity, we have replaced the methylene bridge by a carbonyl group: the amide link between the dye and the crown is stiffer and should preclude pH sensitivity. This carbonyl group is also expected to participate in the complexation, leading to possible additional photophysical effects on cation complexation. Coumarin 343, a very convenient starting material for the synthesis, was chosen instead of coumarin 153.

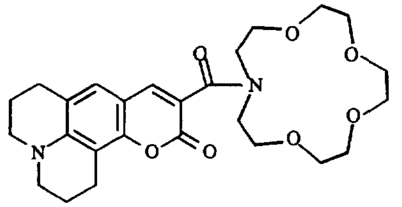

C343-crown

The photophysical and complexing properties of this new fluoroionophore called C343-crown, is the object of this paper with special attention to selectivity and stoichiometry of the complexes.

2. Materials and methods

2.1. Synthesis of C343-crown

One hundred forty microliters (1.1 eq) of thionyl chloride dissolved in 20 ml of dry CH_2Cl_2 were added dropwise to a solution of 500 mg coumarin 343 (Aldrich) dissolved in 20 ml of CH_2Cl_2 containing one drop of dimethylformamide. At the end of the addition, the reaction mixture was refluxed for 30 min. The solvent was partially eliminated by normal pressure distillation: a total volume of ca 40 ml was distilled during which time 20 ml of fresh CH_2Cl_2 were added.

To the mixture, cooled to room temperature, 0.61 ml (2.5 eq) of NEt_3 were added, followed by dropwise introduction of 0.43 g (1.1 eq) of 1-aza-15-crown-5, dissolved in 10 ml of CH_2Cl_2. At the end of the addition, the mixture was refluxed for 30 min and left stirring overnight at room temperature.

The reaction mixture was diluted with 20 ml of CH_2Cl_2 and washed twice with 20 ml of deionized water. After evaporation of the solvent under reduced pressure, the crude product was purified by flash chromatography on silica gel (eluent CH_2Cl_2/MeOH:98/2) affording 520 mg of the desired product which was recrystallized in ethyl acetate. Yield 60%.

Analysis: **M.P.**: 129°C. **RMN**: (500 MHz, $CDCl_3$), δ(ppm): ^{1}H 1.95 (m, 4H) *18* and *21*; 2.73 (t, 2H) *17*; 2.85 (t, 2H) *22*; 3.27 (t, 4 H) *19* and *20*; 3.52 (t, 2H) *10*; 3.58 (t, 2H) and 3.63–3.67 (superimposed t, 10 H) *3–8*; 3.73 (t, 4 H) *1* and *9*; 3.79 (t, 2 H) *2*; 6.84 (s, 1 H) *15*; 7.64 (s, 1H) *13*. ^{13}C 20.07 (*22*); 20.29 (*18*); 21.22 (*21*); 27.36 (*17*); 48.10 (*1*); 49.55 (*19*); 49.94 (*20*); 50.86 (*10*); 68.99 (*2*); 69.96 (*9*); 70.60–71.83 (*3–8*); 106.16 (*23*); 107.51 (*14*); 116.52 (*12*); 118.69 (*16*); 125.46 (*15*); 143.69 (*13*); 146.61 (*26*); 151.91 (*24*); 159.39 (*11*); 167.18 (*25*). **MS** (EI, 70 eV) (m/z): 486 ($M^{\cdot +}$), 458, 354, 284, 268, 218. **FTIR** (KBr pellet) wave number (cm^{-1}): 2931, 2852, 1704, 1621, 1612, 1557, 1508, 1455, 1366, 1307, 1126. **HPLC**: a single peak with 100% peak purity analysis on C18 reversed phase column with MeOH:H_2O (60:40) eluent.

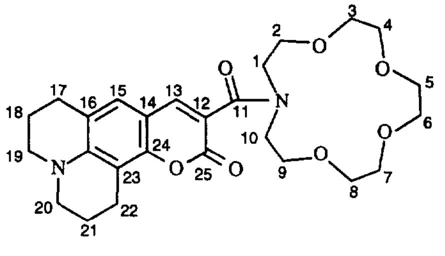

2.2. Solvents and salts

Acetonitrile from Prolabo (Spectronorm®) and ethanol from Carlo Erba (spectrometric grade) were used as solvents for absorption and fluorescence measurements. Lithium, sodium, alkaline-earth perchlorates and potassium thiocyanate purchased from Alfa were of the highest quality available and vacuum dried over P_2O_5 prior to use.

2.3. Apparatus

Infrared spectra were obtained on Perkin-Elmer spectrophotometer (Paragon 1000) using KBr pellet or a 1 mm pathlength cell.

UV–vis absorption spectra were recorded on a Varian Cary 5E spectrophotometer. Corrected emission spectra were obtained on a Spex Fluorolog 1681 spectrofluorimeter. The fluorescence quantum yields were determined using coumarin 504 as a reference ($\Phi = 0.68$ in ethanol) [13].

The excited-state lifetimes were measured at 25°C with our multifrequency (0.1–200 MHz) phase-modulation fluorometer described elsewhere [14]. The samples were excited at 442 nm with a Liconix He–Cd laser and DCM (4-dicyanomethylene-2-methyl-6-*p*-dimethylamino-styryl-4H-pyran) in dimethylsulfoxide was used as a reference ($\tau = 2.130$ ns). The emission wavelength was selected by means of a cut-off filter (GG475). The data were analyzed by the maximum entropy method [15].

3. Results and discussion

3.1. Cation-induced photophysical changes in acetonitrile

Fig. 1 shows the evolution of the absorption and emission spectra of C343-crown on addition of calcium perchlorate in

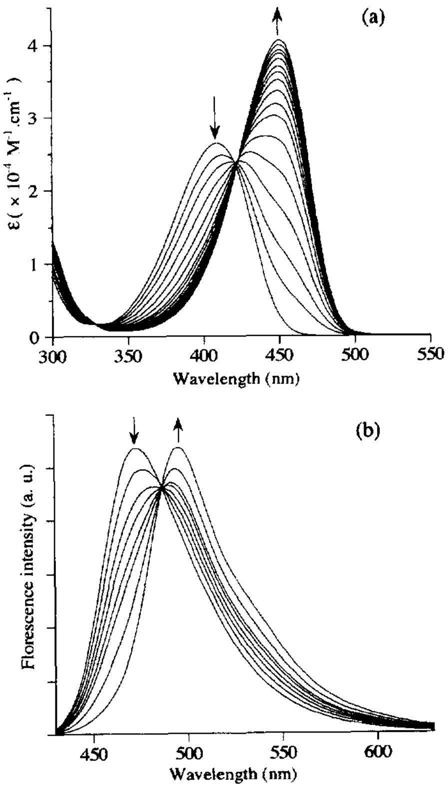

Fig. 1. Evolution of the absorption (A) and fluorescence (B) spectrum of C343-crown in acetonitrile on addition of calcium perchlorate. Excitation wavelength for the fluorescence spectrum: 421 nm (isosbestic point).

acetonitrile. The absorption spectrum undergoes a red shift from 410 to 450 nm at full complexation, whereas the red shift of the emission spectrum is only 10 nm. Similar trends are observed on addition of magnesium perchlorate (Fig. 2). Addition of alkali metal ions (Li^+, Na^+, K^+) induces much weaker effects (see Fig. 3 and Table 1).

The spectral shifts may be understood in the same way as in the case of C153-crown [9], i.e., in terms of cation–dipole interaction because the bound cation interacts with the lactone carbonyl group of the coumarin moiety (Scheme 1).

However, in C343-crown, the carbonyl group of the amide link may also interact with a cation and may contribute to the spectral shift (vide infra).

As in the case of coumarin 153, the dipole moment of coumarin 343 in the excited state is higher than in the ground state as a result of the photoinduced charge transfer from the nitrogen atom of the julolidyl ring to the carbonyl group. Therefore, in the presence of a cation coordinated to this group, the excited state is more stabilized than the ground state so that the absorption and emission spectra are red shifted [4]. The higher the charge density of the cation, the larger the spectral shift, as shown in Table 1.

It should be noted that the increase in the molar absorption coefficient (from 26.8×10^3 for the free ligand to 41.7×10^3 l mol^{-1} cm^{-1} for the calcium complex) is much more pronounced than for C153-crown(O4) (20.3 to 23.3×10^3 l mol^{-1} cm^{-1}) [9] which differs from that of C343-crown only by the bridging group separating the coumarin from the aza crown. Therefore, the large enhancement of the molar absorption coefficient may be related to the fact that the carbonyl group of the amide bridge plays a role in the effects of cation binding on the photophysical properties and may participate in the metal complexation. It is worth examining the molar absorption coefficients of coumarins bearing various electron-withdrawing substituents R in position 3, but with the same structure of the adjacent ring (julolidyl nitrogen atom in position 7). For R = COOH, $COOC_2H_5$, $COCH_3$ and CN, the molar absorption coefficients in methanol are 44.3,

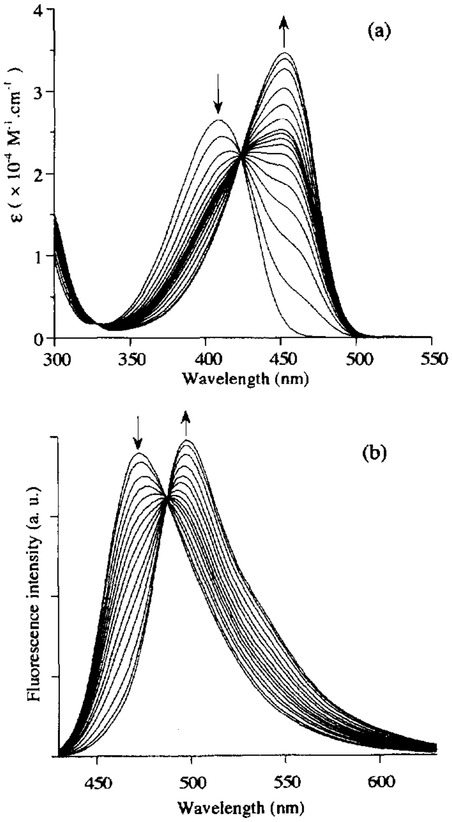

Fig. 2. Evolution of the absorption (A) and fluorescence (B) spectrum of C343-crown in acetonitrile on addition of magnesium perchlorate. Excitation wavelength for the fluorescence spectrum: 425.5 nm (isosbestic point).

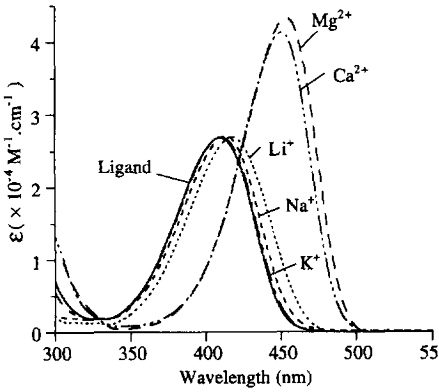

Fig. 3. Absorption spectra of free C343-crown and at full complexation with various cations in acetonitrile.

Table 1
Absorption and fluorescence properties of C343-crown and its complexes with alkali and alkaline–earth metal ions in acetonitrile at room temperature

	Diameter (Å)	Charge density (q Å^{-1})	λ_{abs} (nm)	$\varepsilon \times 10^{-3}$ l mol^{-1} cm^{-1}	λ_{iso} (nm)	λ_{em} (nm)	Φ_F	τ (ns)
Ligand	–	–	410	26.8	–	473	0.56	3.62 ± 0.02
Li^+	1.36	1.47	425.5	25.5	414	487	[a]	[a]
Na^+	1.94	1.03	414	27.1	412	[a]	[a]	[a]
K^+	2.66	0.75	410	26.8	[a]	[a]	[a]	[a]
Mg^{2+}	1.32	3.03	453	43.4	425.5	498	0.57	4.31 ± 0.02
Ca^{2+}	1.98	2.02	450	41.7	421	496	0.56	4.09 ± 0.02

λ_{abs}: absorption maximum; ε: molar absorption coefficient; λ_{iso}: wavelength of the isosbestic point; λ_{em}: emission maximum, Φ_F: fluorescence quantum yield (error: 5–10%), τ: lifetime of the excited state.

[a] The cation-induced changes are too small to yield a reliable value characteristic of the complex.

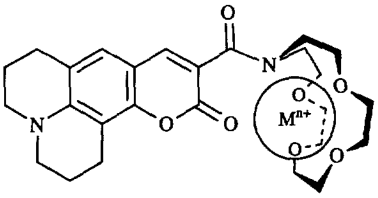

Scheme 1.

46.8, 49.0 and 44.5 × 10^3 l mol^{-1} cm^{-1}, respectively [13]. In our complexes with cations of high charge density (Ca^{2+} and Mg^{2+}), the molar absorption coefficients are close to these values, whereas the coefficient of the free ligand is only slightly higher than that of coumarins having no electron-withdrawing substituent in position 3 (~20 × 10^3 l mol^{-1} cm^{-1}) [13]. This indicates that the amide bridge does not act as an electron-withdrawing substituent in the free ligand, while the electron-withdrawing character of the carbonyl group seems to be recovered when the nitrogen atom strongly interacts with a cation of high charge density.

3.2. Cation-induced photophysical changes in ethanol

In ethanol, the general trends of the changes in photophysical properties on cation binding resemble those in acetonitrile (Fig. 4, Table 2) but the magnitude of the effects is smaller. The effects are again much more pronounced with calcium and magnesium than with lithium, sodium, and potassium. For these cations, there is almost no change in the emission spectrum of the ligand on addition of large amounts of cation.

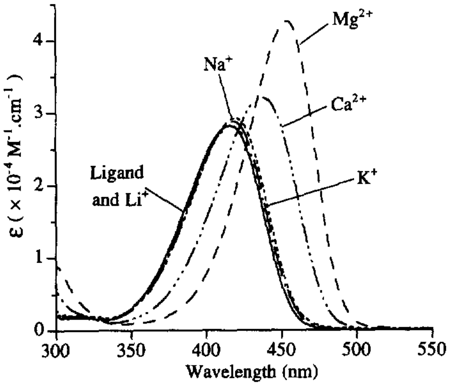

Fig. 4. Absorption spectra of free C343-crown and at full complexation with various cations in ethanol.

3.3. Stoichiometry and stability constant of the complexes

The stability constants can be determined from the variations of either absorbance or fluorescence intensity as a function of cation concentration Table 3.

Table 2
Photophysical properties of C343-crown and its complexes with alkali and alkaline–earth metal ions in ethanol at room temperature

Cation	λ_{abs} (nm)	$\varepsilon \times 10^{-3}$ l mol^{-1} cm^{-1}	λ_{iso} (nm)	λ_{em} (nm)	Φ_F
–	415.5	28.2	–	479	0.66
Li^+	417	28.2	[a]	[a]	[a]
Na^+	419	29.2	[a]	[a]	[a]
K^+	418	28.7	[a]	[a]	[a]
Mg^{2+}	454	42.5	425	495	0.65
Ca^{2+}	437	32.1	421	491	0.63

λ_{abs}: absorption maximum, ε: molar absorption coefficient; λ_{iso}: wavelength of the isosbestic point, Φ_F: fluorescence quantum yield.

[a] The cation-induced changes are too small to yield a reliable value characteristic of the complex.

Table 3
Stability constants of the complexes of C343-crown in acetonitrile and ethanol

Solvent	Cation	log K	
Acetonitrile	Li^+	4.05 ± 0.02[a]	
	Mg^{2+}	4.35 ± 0.1[a]	
	Ca^{2+}	log K_1 = 3.97 ± 0.07	$M + L \rightleftarrows ML$
		log K_2 = 5.32 ± 0.09	$ML + M \rightleftarrows M_2L$
		log K_1 = 4.11 ± 0.07	$M + L \rightleftarrows ML$
		log K_2 = 10.3 ± 0.1	$2\,ML + M \rightleftarrows M_3L_2$
Ethanol	Mg^{2+}	3.43 ± 0.02[a]	
	Ca^{2+}	2.77 ± 0.03[a]	

[a] Stoichiometry of the complex: 1:1.

In the case of a stoichiometry 1:1, the stability constant K_1 which controls the equilibrium between the free ligand L and the complex ML,

$$M+L \rightleftarrows ML$$

can be written as

$$K_1=\frac{[ML]}{[L][M]}$$

where [L], [M], [ML] are the concentrations of free ligand, free metal ion and complex, respectively.

It is easy to derive the following equation [9]:

$$X=X_0+\frac{X_{\lim}-X_0}{2c_L}[c_L+c_M+1/K_1 -[(c_L+c_M+1/K_1)^2-4\,c_Lc_M]^{1/2}] \qquad (1)$$

where X is the absorbance or the fluorescence intensity of the solution. X_0 and $X_{\lim}$ are the values of X for the free ligand and of the ML complex, respectively. c_L and c_M are the total concentrations of ligand and metal ion, respectively. K_1 can thus be obtained by using Eq. (1) and a nonlinear least-squares analysis of X vs. c_M. If $X_{\lim}$ cannot be accurately determined, it can be left as a floating parameter in the analysis.

Apart from the case of complexation by calcium in acetonitrile (vide infra), all the titration curves can be satisfactorily fitted to Eq. (1), in which $X_{\lim}$ and K_1 are left as floating parameters. An example of titration curve is given in Fig. 5 for magnesium, and the results are reported in Table 4 for lithium, calcium and magnesium complexes. For the other cations, the photophysical changes are too small for a reliable determination of the stability constants which are likely to be much smaller.

In the case of calcium complexes in acetonitrile, curve fitting with Eq. (1) was not satisfactory. Successive complexations according to the following scheme were then considered:

$$M+L \rightleftarrows ML \quad K_1=\frac{[ML]}{[L][M]}$$

$$ML+M \rightleftarrows M_2L \quad K_2=\frac{[M_2L]}{[ML][M]}$$

The following equation can be derived (see Appendix A):

$$X=\frac{X_0+c_LbK_1[M]+X_{\lim}\beta[M]^2}{1+K_1[M]+\beta[M]^2} \qquad (2)$$

where $\beta=K_1K_2$ and b is a parameter which includes the molar absorption coefficient (and quantum yield) of the intermediate complex ML. This relatively simple expression can be used under the approximation $[M]\cong c_M$. K_1 and b can be determined by a nonlinear least-squares analysis of X vs. c_M. $X_{\lim}$ is also left as a floating parameter in the analysis, if necessary. It should be noted that there is no explicit expression of X vs. c_M if the approximation $[M]\,\tilde{}\,c_M$ is not valid.

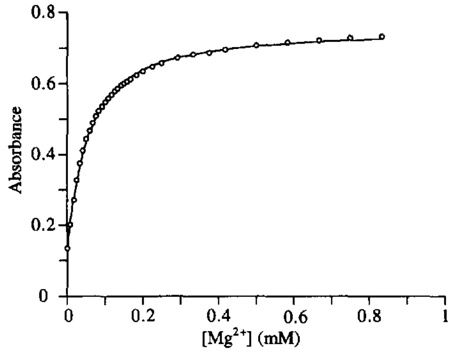

Fig. 5. Variations in absorbance (○) at 453 nm of a solution of C343-crown in acetonitrile (5.18×10^{-5} M) as a function of magnesium perchlorate concentration. The solid line represents the best fit with Eq. (1). The correlation coefficient is 0.9995.

The titration curve is consistent with the above model, as shown by the satisfactory fit with Eq. (2) (see Fig. 6a). The successive equilibrium constants are $K_1=9.4\times10^3\pm1.5\times10^3$ and $K_2=2.1\times10^5\pm0.5\times10^5$ M^{-1}. A binuclear complex is hard to imagine: the first cation on one side of the crown may interact with the lactone carbonyl group, while the second one, on the other side of the crown interacts with the carbonyl group of the amide bridge. The fact that the second stability constant is more than 20 times larger than the first one would be indicative of a cooperative effect and it seems difficult to interpret such a cooperative binding.

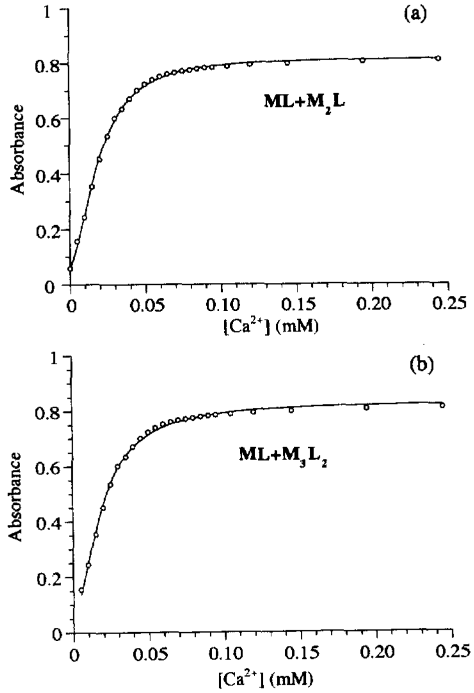

Fig. 6. Variations in absorbance (○) at 450 nm of a solution of C343-crown in acetonitrile (2×10^{-5} M) as a function of calcium perchlorate concentration. The solid line represents in (A) the best fit with Eq. (2) corresponding to successive complexes ML and M_2L (correlation coefficient: 0.9996), and in (B) the best fit with Eq. (3) corresponding to successive complexes Ml and M_3L_2 (correlation coefficient: 0.9990).

Another hypothesis has also been tested for the calcium complexes with the following successive complexations:

$$M+L\rightleftarrows ML \quad K_1=\frac{[ML]}{[L][M]}$$

$$2ML+M\rightleftarrows M_3L_2 \quad K_2=\frac{[M_3L_2]}{[ML]^2[M]}$$

From these equilibria, the following equation was derived (see Appendix B):

$$X=\frac{N}{4K_1^2K_2[M]^3c_L}\left(X_0+bc_LK_1[M]+\frac{X_{\lim}N}{2}\right) \qquad (3)$$

in which

$$N=-1-K_1[M]+\{(1+K_1[M])^2+8c_LK_1^2K_2[M]^3\}^{1/2}$$

The results fit very well with this more complex expression (Fig. 6b) used as in the preceding case under the approximation $[M]\cong c_M$ and no significant difference may be found between the quality of the fits made according to Eq. (2) or Eq. (3) (see Fig. 6). The successive equilibrium constants are found to be $K_1=1.3\times10^4\pm0.2\times10^4$ M^{-1} and $K_2=2.1\times10^{10}\pm0.5\times10^{10}$ M^{-2}. Even if no significant mathematical discrimination is available, the second model seems to be more reasonable than the preceding one if the M_3L_2 complex is presented with a calcium cation in each aza crown pocket while the four carbonyl groups of the two coumarins coordinate to a third calcium ion as in an EDTA system (Scheme 2).

Information on the structure of complexes with crown ethers can be drawn from X-ray crystallography, but up to now it turned out to be impossible to crystallize the complex. Fourier-transform infrared spectra of the free ligand and of its complex with calcium or magnesium perchlorate in deuterated acetonitrile were recorded. Deuterated acetonitrile was preferred to acetonitrile due to its very weak absorption between ca. 1400 and 1750 cm^{-1} where carbonyl groups absorb. For the free ligand, two carbonyl absorption bands are observed, at 1706 cm^{-1} for the lactone and 1619 cm^{-1} for the amide link. At a molar ratio of ca 1:12 between C343-crown and $Mg(ClO_4)_2$, corresponding to the full complexation, these bands are respectively shifted to 1669 cm^{-1} and 1610 cm^{-1}. A similar effect is observed with $Ca(ClO_4)_2$ at a molar ratio corresponding to the 1:1 complex. At high calcium concentration (molar ratio ca 1:15), the bands remain shifted to 1669 cm^{-1} and 1610 cm^{-1} for the lactone and the amide C=O, respectively, but a new band appears at 1649 cm^{-1}.

The large shift (37 cm^{-1}) observed for the lactone C=O band upon complexation by magnesium and calcium cations is a clear second evidence of the participation of this carbonyl to the metal complexation. On the other hand, the amide C=O band is only weakly shifted by the complexation and thus probably does not play a significant role in chelation of the metal. The new band observed at high calcium concentration is still unexplained but could be the indication for a more complicated structure than a M_2L complex, giving further argument for an assembly like M_3L_2.

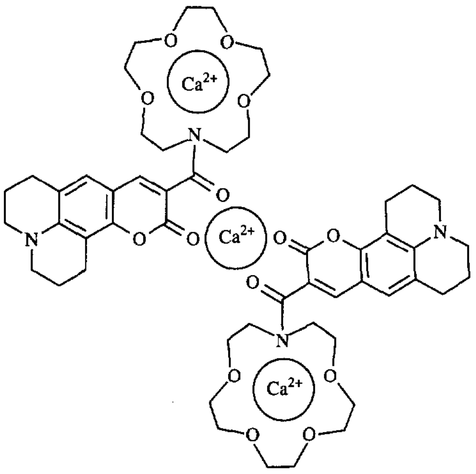

Scheme 2.

4. Conclusion

As compared with C153-crown, the replacement of the methylene bridge by an amide bridge in C343-crown leads to interesting improvements. First of all, the selectivity towards alkaline earth–metal ions with respect to alkaline cations is much better, but the selectivity between calcium and magnesium is to be improved. Moreover, additional photophysical effects result from the presence of the amide function: when the aza crown is occupied by a cation, the linking amide behaves as an electron withdrawing group and generates hyperchromicity as well as additional spectral shifts.

Acknowledgements

We acknowledge Mr. Jean-Pierre Lefèvre (CNAM, ENS-Cachan), Mr. Claude Drossart (Université de Louvain) and Dr. Roland Touillaux (Université de Louvain) for assistance with the lifetime, FTIR, and NMR measurements, respectively. The Belgian FNRS and french CNRS institutions are thanked for financial support. JLHJ is 'Chercheur qualifié' from the FNRS.

Appendix A

Let us consider the following successive complexations:

$$M+L\rightleftarrows ML \quad K_1=\frac{[ML]}{[L][M]} \qquad (4)$$

$$ML+M\rightleftarrows M_2L \quad K_2=\frac{[M_2L]}{[ML][M]} \qquad (5)$$

The measurements are performed under conditions where the absorbance or the fluorescence intensity of the free ligand X_0 is proportional to the ligand concentration c_L:

$$X_0=a\,c_L \tag{6}$$

After addition of a given amount of salt at a concentration c_M, the absorbance or the fluorescence intensity becomes

$$X=a[L]+b[ML]+c[M_2L] \tag{7}$$

Parameters a, b, c include the molar absorption coefficient (and quantum yield) of L, ML, M_2L, respectively.

Mass conservation can be expressed for the ligand and the metal ion as follows:

$$c_L=[L]+[ML]+[M_2L] \tag{8}$$

$$c_M=[M]+[ML]+2[M_2L] \tag{9}$$

In the presence of an excess of metal ion so that the ligand is fully complexed, X reaches the limiting value X_{lim}:

$$X_{lim}=c\,c_L \tag{9a}$$

From Eqs. (3)–(9), it is easy to show that X can be written in the form of Eq. (2).

Appendix B

When considering the complexations:

$$M+L\rightleftarrows ML \quad K_1=\frac{[ML]}{[L][M]} \tag{4a}$$

$$2ML+M\rightleftarrows M_3L_2 \quad K_2=\frac{[M_3L_2]}{[ML]^2[M]} \tag{10}$$

Using the following relation,

$$c_L=[L]+[ML]+2[M_3L_2] \tag{11}$$

it is easy to show that

$$2K_1^2K_2[M]^3[L]^2+(1+K_1[M])[L]-c_L=0 \tag{12}$$

Eq. (6) is still valid and the limiting value X_{lim} becomes

$$X_{lim}=c\,c_L/2 \tag{13}$$

During the intermediate steps of cation addition, the absorbance can be expressed as

$$X=a[L]+bK_1[M][L]+cK_1^2K_2[M]^3[L]^2 \tag{14}$$

Using Eqs. (6) and (13) and introducing into Eq. (14) the expression of $[L]$ obtained by solving Eq. (12), we obtain the final Eq. (3).

References

[1] A.W. Czarnik (Ed.), Fluorescent Chemosensors for Ion and Molecule Recognition, A.C.S. Symposium series 538, Am. Chem. Soc., Washington DC, 1992.

[2] J.R. Lakowicz (Ed.), Topics in fluorescence spectroscopy, Volume 4: Probe Design and Chemical Sensing, Plenum, New York, 1994.

[3] J.-P. Desvergne, A.W. Czarnik (Eds.), Chemosensors of Ion and Molecule Recognition, NATO ASI series, Kluwer Academic Publishers, Dordrecht, 1997.

[4] B. Valeur, Principles of fluorescent probe design for ion recognition, in: J.R. Lakowicz (Ed.), Topics in Fluorescence Spectroscopy, Probe Design And Chemical Sensing, Vol. 4, Plenum, New York, 1994, pp. 21–48.

[5] R.A. Bissell, A.P. de Silva, H.Q. Nimal Gunaratne, P.L. Mark Lynch, G.E.M. Maguire, C.P. McCoy, K.R.A. Samankumara Sandanayake, Fluorescent PET, photoinduced electron transfer, sensors, Top. Curr. Chem. 168 (1993) 223.

[6] B. Valeur, J. Bourson, J. Pouget, in: A.W. Czarnik (Ed.), Fluorescent Chemosensors for Ion and Molecule Recognition, A.C.S. Symposium Series 538, Am. Chem. Soc., Washington DC, 1992, pp. 25–44.

[7] H. Bouas-Laurent, J.-P. Desvergne, F. Fages, P. Marsau, in: A.W. Czarnik (Ed.), Fluorescent Chemosensors for Ion and Molecule Recognition, A.C.S. Symposium series 538, Am. Chem. Soc., Washington, DC, 1992, pp. 59–73.

[8] J. Bourson, M.N. Borrel, B. Valeur, Anal. Chim. Acta 257 (1992) 189.

[9] J. Bourson, J. Pouget, B. Valeur, J. Phys. Chem. 97 (1993) 4552.

[10] J. Bourson, F. Badaoui, B. Valeur, J. Fluorescence 4 (1994) 275.

[11] F. Badaoui, J. Bourson, Anal. Chim. Acta 302 (1995) 341.

[12] B. Valeur, F. Badaoui, E. Bardez, J. Bourson, P. Boutin, A. Chatelain, I. Devol, B. Larrey, J.P. Lefevre, A. Soulet, in: J.-P. Desvergne, A.W. Czarnik (Eds.), Chemosensors of Ion and Molecule Recognition, NATO ASI series, Kluwer Academic Publishers, Dordrecht, 1997, pp. 195–220.

[13] G.A. Reynolds, K.H. Drexhage, Opt. Commun. 13 (1975) 222.

[14] J. Pouget, J. Mugnier, B. Valeur, J. Phys. E Sci. Instr. 22 (1989) 855.

[15] J.C. Brochon, A.K. Livesey, J. Pouget, B. Valeur, Chem. Phys. Lett. 174 (1990) 517.